Deployable Tensegrity Lunar Tower

Muhao Chen[1], Raman Goyal[1], Manoranjan Majji[2] and Robert E. Skelton[3]

[1]Graduate Student, Department of Aerospace Engineering, Texas A&M University, TX, USA; emails: muhaochen@tamu.edu, ramaniitrgoyal92@tamu.edu
[2]Assistant Professor, Department of Aerospace Engineering, Texas A&M University, TX, USA; email: mmajji@tamu.edu
[3]TEES Eminent Research Professor, Department of Aerospace Engineering, Texas A&M University, TX, USA; email: bobskelton@tamu.edu

ABSTRACT

A tensegrity tower design to support a given payload for the moon mining operation is proposed in this paper. A non-linear optimization problem for the minimal-mass structure design is posed and solved, subject to the yielding constraints for strings and yielding and buckling constraints for bars in the presence of lunar gravity. The optimization variables for this non-linear problem are structural complexity and pre-stress in the strings. Apart from local failure constraints of yielding and buckling, global buckling is also considered. The structure designed as a deployable tower is a T_nD_1 tensegrity structure. A case study demonstrates the feasibility and advantage of the tower design. The principles developed in this paper are also applicable for building other structures on the Earth or other planets.

INTRODUCTION

The great heroic success of the Apollo program has triggered a strong will, passion, and enthusiasm of the public. Till now, humans have developed various heavy rockets, put rovers on other planets, sent people to ISS, and launched probes to the Sun. The interest is now returning to the moon to utilize its abundant resources. Various Lunar exploration missions have provided us with information about its abundant useful resources. For example, the entire lunar surface is covered with an unconsolidated layer of regolith (Heiken et al. 1991), which can be used as a very efficient material for building space habitat shields (Chen et al. 2018; Chen et al. 2020a). The moon is especially rich in Ca, Al, Si, O, Mg, Fe, and Ti (Crawford 2015). The recent study also shows that a large amount of ice has a permanent presence in the shadowed lunar polar craters (Spudis et al. 2013). The goal of this paper is to study a feasible design of a lightweight tower to support moon mining operations.

Scientists have been exploring the idea of mining the moon for some time. Mining ice on the moon can be achieved by using solar energy to heat the ice and store it as water (Duke et al. 1998). Rock breakage by microwave techniques, mineral processing, and materials manufacturing for ISRU have also been discussed (Tukkaraja et al. 2018). Tunnel Boring Machines could offer another safe and efficient approach for mining on the moon (Rostami et al. 2018). Sanders presented NASA's lunar ISRU strategy, which includes plans for regolith, polar water/volatile mining, commercial opportunities, rovers, and mission schedules (Sanders 2019). The mining design of these works mainly focuses on rovers, operations, and extracting minerals. Some of the important issues are left unsolved for mining in the permanent shaded polar craters at the high latitude of the moon: 1) a structure to help collect and distribute solar energy efficiently (mirrors and solar panels to light up the operation area, store energy, and generate heat) and 2) supporting communication equipment. All these problems lead to the requirement of a lunar tower. As mass is one of the most critical issues for space exploration, we desire to design a minimal mass deployable lunar tower.

Tensegrity system is a subset of multi-body systems, which includes cylindrical rigid bodies (bars) and elastic members (strings) arranged in a stabilizable topology (Chen and Skelton 2020). The tensegrity art-form was first created by Ioganson (1921) and Snelson (1948), and the word 'Tensegrity' was coined as 'Tensile + Integrity = Tensegrity' by Buckminster Fuller (Fuller 1959). After decades of study, tensegrity structures have shown their great advantage in designing lightweight structures (Ma et al. 2020). Tensegrity system, as a new dimension of engineering thought, motivates engineers to rethink and study structures in a more fundamental way, for example, the mechanical response of 3D tensegrity lattices (Rimoli and Pal 2017), minimum mass bridges (Fabbrocino et al. 2017), high-performance robotics (Bliss et al. 2012), robot locomotion (Wang et al. 2020), morphing airfoil (Shen et al. 2020), lander (Booth et al. 2020; SunSpiral et al. 2013; Chen et al. 2017; Goyal et al. 2018; Zhao and Hernandez 2019), tensegrity spine (Sabelhaus et al. 2017), and perhaps biology shows the great evidence that tensegrity should be the way to design structures (Skelton and de Oliveira 2009). Sultan and Skelton gave a deployable tensegrity tower based on a multi-stage three-strut Snelson-type tensegrity topology (Sultan and Skelton 2003). Schlaich built probably the tallest tower (62.3 m, consists of 6 three-strut Snelson-type tensegrity unit, each unit 8.3 m) (Schlaich 2004). Yildiz and Lesieutre studied stiffness properties and deployable strategies of a class-1 and class-2 Snelson-type tower (Yildiz and Lesieutre 2018; Yildiz and Lesieutre 2019). However, none of these towers gives a complete description of the minimal mass deployable tower design in the presence of gravity. This paper utilizes the tensegrity paradigm to design a tower for lunar mining, requiring less mass to meet load constraints. The principles developed in this paper can also be used for other tensegrity structure designs.

This paper is organized as follows: Section 1 provides motivation and introduction of the lunar tower design for mining on the moon. Section 2 derives the minimum mass tensegrity principles, including statics analysis, structure mass formulation, gravitational forces, and global stability analysis. To solve the nonlinear optimization problem, an iterative algorithm is also provided. Section 3 describes the deployable $T_n D_1$ tower design, which is a combination of T-Bar and D-Bar systems, and Section 4 presents a case study detailing the results of minimum mass design. Section 5 provides a concise summary of the research work.

MINIMAL MASS TENSEGRITY PRINCIPLES

Static Analysis for Tensegrity Structures

The static equilibrium equation for a given tensegrity structure and given external force can be written as (Goyal and Skelton 2019):

$$NK = W,\ K = C_s^{\mathsf{T}} \hat{\gamma} C_s - C_b^{\mathsf{T}} \hat{\lambda} C_b, \tag{1}$$

where $N \in R^{3\times n}$ is the nodal matrix with each column of N representing the node position, n is number of nodes, and, $C_s \in R^{\alpha\times n}$ and $C_b \in R^{\beta\times n}$ are the connectivity matrices of strings and bars (with 0, -1, and 1 contained in each row), respectively. The number of bars and strings are denoted by α and β. The external force matrix $W \in R^{3\times n}$ contains each of its column as the force vector acting on the corresponding node, $\gamma \in R^{\alpha\times 1}$ is a vector of force densities (force per unit length) in the strings, and $\hat{v}$ is a diagonal matrix of the elements of a vector v. The string and bar vectors are contained in the string matrix $S = \begin{bmatrix} s_1 & s_2 & \cdots & s_\alpha \end{bmatrix} \in R^{3\times\alpha}$ and in the bar matrix $B = \begin{bmatrix} b_1 & b_2 & \cdots & b_\beta \end{bmatrix} \in R^{3\times\beta}$ respectively, such as $S = NC_s^T$ and $B = NC_b^T$. Let us take the i^{th} column of Eq. (1):

$$S\hat{\gamma} C_s e_i - B\hat{\lambda} C_b e_i = We_i, \tag{2}$$

where $e_i = [0\ 0\ \cdots\ 1\ \cdots\ 0\ 0]^T$ is a column with 1 as the i^{th} element and zeros elsewhere. Using the identity $\hat{x}y = \hat{y}x$, for x and y being column vectors, we can write the previous equation as:

$$S\widehat{(C_s e_i)}\gamma - B\widehat{(C_b e_i)}\lambda = We_i. \tag{3}$$

Stacking all the columns from $i = 1$ to $i = n^{\text{th}}$ column, we get:

$$Ax = W_{vec},\ x = \begin{bmatrix} \gamma^T & \lambda^T \end{bmatrix}^T, \tag{4}$$

where:

$$A = \begin{bmatrix} \widehat{S(C_s e_1)} & -\widehat{B(C_b e_1)} \\ \widehat{S(C_s e_2)} & -\widehat{B(C_b e_2)} \\ \vdots & \vdots \\ \widehat{S(C_s e_n)} & -\widehat{B(C_b e_n)} \end{bmatrix}, \; W_{vec} = \begin{bmatrix} We_1 \\ We_2 \\ \vdots \\ We_n \end{bmatrix}. \tag{5}$$

Mass Formulation for Tensegrity Structures

The strings can fail by material yielding while bars can fail by both yielding and buckling. The minimum mass of the structure is obtained when all the strings are designed to their yield point and all the bars are designed at the onset of yielding or buckling:

$$M = \frac{\rho_s}{\sigma_s} \sum_{i=1}^{\alpha} \gamma_i ||s_i||^2 + \sum_{j=1}^{\beta} \max \left(\frac{\rho_b}{\sigma_b} \lambda_j ||b_j||^2, 2\rho_b \lambda_j^{\frac{1}{2}} \left(\frac{||b_j||^5}{\pi E_b} \right)^{\frac{1}{2}} \right), \tag{6}$$

where ρ_s, ρ_b, σ_s, σ_b are the density and yield strength of strings and bars, respectively. The length of each string and each bar are denoted by $||s_i||$, and $||b_j||$ for $i = 1, 2, \cdots, \alpha$; and $j = 1, 2, \cdots, \beta$, and E_b is Young's modulus of bars. As seen from Eq. (6), the maximum of mass required for yielding and buckling is considered for each bar.

Let us define a label matrix $Q \in R^{\beta \times \beta}$ as:

$$Q_{jj} = \begin{cases} 0; & \lambda_j \geq \dfrac{4\sigma_b^2 ||b_j||}{\pi E_b}, \text{ bar yields} \\ 1; & \lambda_j < \dfrac{4\sigma_b^2 ||b_j||}{\pi E_b}, \text{ bar buckles} \end{cases}, \tag{7}$$

and the off diagonal elements of Q are zeros. This matrix is used to identify whether a bar is yielding or buckling. Notice that a simple operation of $(I - Q)$ works intuitively for representing the bar under yielding constraint. The bars are now separated into two types and the minimal mass formula can be well defined in matrix form (Goyal et al. 2019):

$$\begin{aligned} M = & \frac{\rho_s}{\sigma_s} (vec(\lfloor S^T S \rfloor))^T \gamma + \frac{\rho_b}{\sigma_b} (vec(\lfloor B^T B \rfloor (I - Q)))^T \lambda \\ & + \frac{2\rho_b}{\sqrt{\pi E_b}} (vec(\lfloor B^T B \rfloor^{\frac{5}{4}} Q))^T \lambda^{\frac{1}{2}}, \end{aligned} \tag{8}$$

where $\lfloor \bullet \rfloor$ is an operator taking the diagonal elements of a matrix, $vec(\bullet)$ is an operator taking the elements of the matrix and form a vector.

Tensegrity Statics in the Presence of Gravity

Since gravity is unlike a given set of specific external forces that apply to the structure, it is determined by the mass of the structure itself. In other words, the statics mass optimization process is coupled with the gravity force. The total force W can be separated into two parts $W = W_e + W_g$, where W_g is the gravity force, and W_e is other applied external force. The acceleration due to gravity is defined as $\boldsymbol{g}$ with lunar gravity as $\boldsymbol{g}_{moon} = \begin{bmatrix} 0 & 0 & -1.62 \end{bmatrix}^T$ m/s^2. The gravity force can be modeled by lumped forces equally distributed on the member nodes (Nagase and Skelton 2014). Thus, the gravitational force due to bars and strings can be expressed as:

$$W_{gi} = \frac{1}{2}\boldsymbol{g}\frac{\rho_s}{\sigma_s}\left(vec(\lfloor S^T S \rfloor)\right)^T \widehat{|C_s e_i|}\gamma + \frac{1}{2}\boldsymbol{g}\frac{\rho_b}{\sigma_b}\left(vec(\lfloor B^T B \rfloor (I - Q))\right)^T \widehat{|C_b e_i|}\lambda$$

$$+ \frac{1}{2}\boldsymbol{g}\frac{2\rho_b}{\sqrt{\pi E_b}}\left(vec(\lfloor B^T B \rfloor^{\frac{5}{4}} Q)\right)^T \widehat{|C_b e_i|}\lambda^{\frac{1}{2}}, \tag{9}$$

where $| \bullet |$ is an operator getting the absolute value of each element for a given matrix. Stacking all the columns, we get:

$$W_{g\ vec} = \begin{bmatrix} W_{g1}^T & \cdots & W_{gi}^T & \cdots & W_{gn}^T \end{bmatrix}^T. \tag{10}$$

Global Stiffness Matrix for Tensegrity Structures

Consider a small variation around the equilibrium position as:

$$N + dN = \begin{bmatrix} \cdots & (n_k + dn_k) & \cdots \end{bmatrix},\ W + dW = \begin{bmatrix} \cdots & (w_k + dw_k) & \cdots \end{bmatrix}, \tag{11}$$

$$\gamma + d\gamma = \begin{bmatrix} \cdots & (\gamma_i + d\gamma_i) & \cdots \end{bmatrix}^T,\ \lambda + d\lambda = \begin{bmatrix} \cdots & (\lambda_j + d\lambda_j) & \cdots \end{bmatrix}^T, \tag{12}$$

and write the statics equation about the equilibrium as (Nagase and Skelton 2014):

$$(N + dN)C_s^T \widehat{(\gamma + d\gamma)} C_s - (N + dN)C_b^T \widehat{(\lambda + d\lambda)} C_b = W + dW. \tag{13}$$

We assume the materials are Hookean and therefore the force densities (string in tension, bar in compression) can be expressed as:

$$\gamma_i = k_{si}\left(1 - \frac{||s_{i0}||}{||s_i||}\right),\ \lambda_j = -k_{bj}\left(1 - \frac{||b_{j0}||}{||b_j||}\right), \tag{14}$$

where $||s_{i0}||$ and $||b_{j0}||$ are the rest length of the i^{th} string and j^{th} bar. The spring constants of strings and bars, k_{si} and k_{bj} satisfy:

$$k_{si} = \frac{E_{si}A_{si}}{||s_{i0}||},\ k_{bj} = \frac{E_{bj}A_{bj}}{||b_{j0}||}, \tag{15}$$

where A_{si} and A_{bj} are cross-section areas, E_{si} and E_{bj} are Young's modules of the strings and bars. With the information of label matrix Q, mass of a string and a bar are given as:

$$m_{si} = \frac{\rho_s}{\sigma_s}||s_i||^2\gamma_i,\ m_{bj} = (1-Q_{jj})\frac{\rho_b}{\sigma_b}||b_j||^2\lambda_j + Q_{jj}\frac{2\rho_b}{\sqrt{\pi E_{bj}}}||b_j||^{\frac{5}{2}}\lambda_j^{\frac{1}{2}}. \tag{16}$$

Rearrange Eqs. (13-16), we get the stiffness matrix K_n for tensegrity structure subject to yielding and buckling constraints as:

$$K_n vec(dN) = vec(dW), \tag{17}$$

where

$$\begin{aligned} K_n = &(C_s^T \otimes I_3)\mathbf{b.d.(}K_{s1}\mathbf{,}\cdots\mathbf{,}K_{s\alpha})(C_s \otimes I_3) \\ &- (C_b^T \otimes I_3)\mathbf{b.d.(}K_{b1}\mathbf{,}\ \cdots\mathbf{,}\ K_{b\beta})(C_b \otimes I_3), \end{aligned} \tag{18}$$

and

$$\begin{aligned} K_{si} &= \gamma_i\left(I_3 + \frac{E_{si}}{\sigma_s}\frac{s_i s_i^T}{||s_i||^2}\right), \\ K_{bj} &= \lambda_j\left(I_3 - (1-Q_{jj})\frac{E_{bj}}{\sigma_b}\frac{b_j b_j^T}{||b_j||^2}\right) - 2Q_{jj}\sqrt{\frac{E_{bj}}{\pi}}\frac{b_j b_j^T}{||b_j||^{\frac{3}{2}}}\lambda_j^{\frac{1}{2}}. \end{aligned} \tag{19}$$

Algorithm for Minimal Mass Tensegrity Structure

The minimal mass problems can be formulated as:

$$\begin{cases} \underset{x}{\text{minimize}} & M \\ \text{subject to} & Ax = W_{e\ vec} + W_{g\ vec},\ x \geq \epsilon_0, \text{and } eig(K_n) > \mu I \end{cases}, \tag{20}$$

where ϵ_0 is the prestress assigned to the strings, and $\epsilon_0 \geq 0$ guarantees that all strings are in tension and all bars in compression, $eig(K_n)$ returns the eigenvalues of the matrix K_n, and the system is globally stable at the equilibrium for $\mu \geq 0$. Notice that to solve Eq. (20), one needs to specify the label matrix Q. However, one cannot exactly tell Q for any structure in advance because it is determined by structure topology and external force. To obtain a global solution, the nonlinear optimization problem can be solved in an iterative manner as described in Algorithm 1.

DEPLOYABLE TOWER DESIGN

Algorithm 1: Minimal Mass Tensegrity subject to Stability and Gravity

1) Let $Q = I^{\beta\times\beta}$, $W_{g\ vec} = 0$, $\epsilon_0 = 0$, $\delta\epsilon = 0.01$, $\mu = 0$.
2) Compute force densities x:
while $\min\{eig(K_n)\} < \mu$ **do**
  while $Q_{i+1} \neq Q_i$ **do**

$$\begin{cases} \underset{x}{\text{minimize}}\ M \\ \text{subject to } Ax = W_{e\ vec} + W_{g\ vec},\ x \geq \epsilon_0. \end{cases}$$

    Compute λ from x, check Eq. (7), update Q.
    Update $W_{g\ vec}$ from Eq. (9).
    $i \leftarrow i + 1$.
  end while
  Compute stiffness matrix K_n from Eq. (18).
  $\epsilon_0 \leftarrow \epsilon_0 + \delta\epsilon$.
end while
.

T-Bar Structure

Skelton and de Oliveira have proved that T-Bar and D-Bar systems require less mass than a continuum bar in taking the same compression load $f(l_0)$. A three-dimensional T-Bar unit is shown in Figure 1a (Skelton and de Oliveira 2009). Each longitudinal bar in the T-bar structure can be replaced with another T-bar tensegrity unit while preserving the total length of the structure. Repeating this self-similar process q times is defined as the complexity of the structure. Figure 2a shows a T-Bar structure of complexity $q = 3$.

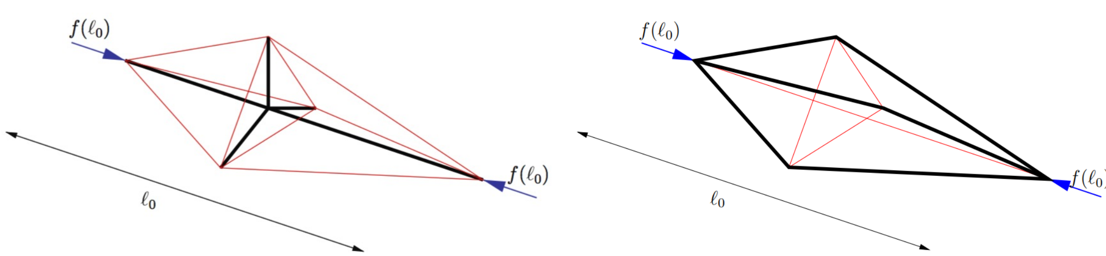

(a) 3D T-Bar unit. (b) 3D D-Bar unit.

Figure 1: Three-dimensional tensegrity T-Bar and D-Bar unit, black lines are bars and red lines are strings.

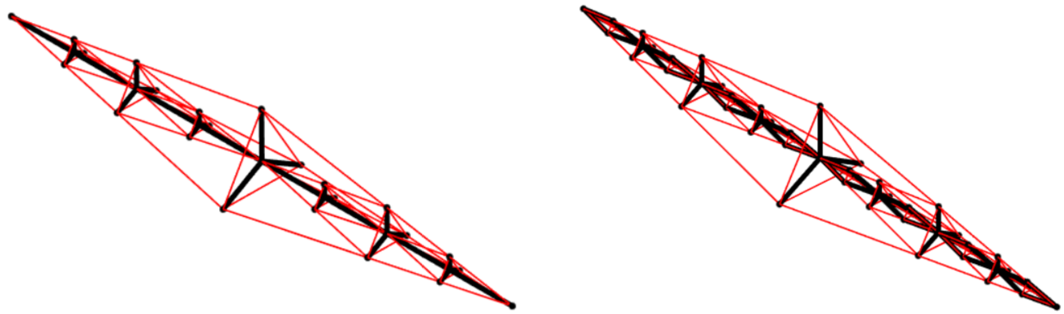

(a) Three-dimensional T_3 structure. (b) Three-dimensional T_3D_1 structure.

Figure 2: Three-dimensional tensegrity T-Bar and T_nD_1-Bar structure.

D-Bar Structure

The dual of the T-Bar unit is called a D-Bar structure, which is shown in Figure 1b. The D-bar is also shown to be a more efficient structure in taking a compressive load than a continuum bar (Skelton and de Oliveira 2009). Another advantage of the D-bar structure is its deployability. The length of the structure can be changed by controlling the length of the individual strings.

Tensegrity Tower Design

We combine the two structures such that it is both deployable and mass efficient in taking compression. Let us start with a T-Bar structure with complexity $q = n$ and replace its each 2^n longitudinal bars with D-Bar units of complexity 1 to obtain a T_nD_1 structure. A 3-dimensional T_3D_1 is shown in Figure 2b. The same T_nD_1 structure is used to design towers as the payload on top of the tower will exert a compressive load on two ends of the structure. The simulation and experimental model is shown in Figure 3.

Tower Deployment Discussion

Our NIAC (NASA Innovative Advanced Concepts) phase I project with Joel Sercel on lunar-polar propellant mining outpost (LPMO): affordable exploration and industrialization, gives a deployable experimental model, shown in Figure 3b. The metal materials for bars are available on the moon (Schrunk et al. 2007), the strings (for example, UHMWPE, Ultra High Molecular Weight Polyethylene) can be shipped from the earth. There are mainly two ways to deploy tensegrity structures: 1. Altering string rest-lengths, which are usually realized by a motor pulley cable system (Abdallah et al. 2012; Sultan 2014). 2. Using shape memory alloy (SMA) tendon wires, which are usually achieved by SMA and DC current supply devices (Bundhoo et al. 2009; Kim et al. 2016). The first method has these properties: wider control bandwidth, less cost, more environmentally robust, but

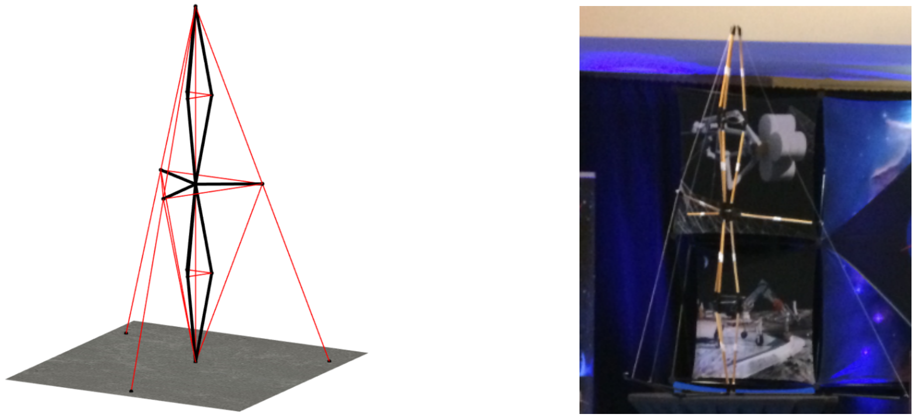

(a) Mathematical tower model.

(b) Experimental tower model.

Figure 3: Three-dimensional T_2D_1 tensegrity tower models, source of (b): http://www.leonarddavid.com/lunar-polar-propellant-mining-outpost-envisioned/.

mechanically more complicated than the second one. For this tower design, the deployability can be achieved by shorting the middle string length of the D-Bar. A shape control algorithm for class-k tensegrity (Chen et al. 2020b) can be applied to get the deploy sequence, shown in Figure 4.

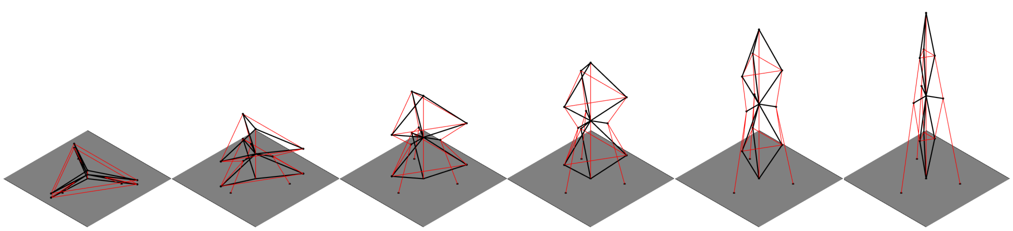

Figure 4: Tower deployment from a stowed configuration to a fully deployable one.

CASE STUDY

The lunar craters vary in size from a few meters to 400 km, the depth of the craters are from less than 1 meter to 8 km, and a large portion of these craters is around 10 km in diameter and 2 km deep (Pike 1974). Here, we present a 2 km tall tower design, but the process developed in this paper is applicable for designing towers of any height. The payloads on the top of the tower include solar panels, communication devices, and mirrors with an estimated load of $m_p = 6{,}000$ kg. Therefore, the compressive force at the top of the tower is $F = m_p g_{moon} = 6,000 \times 1.62$ N $= 9,720$ N. We use carbon-fiber rods for bars and UHMWPE for strings. The material properties are given in Table 1.

Table 1: Material property for bars and strings.

Properties	Carbon-Rod	UHMWPE-String	Units
Yield Stress	1.72×10^9	2.70×10^9	Pa
Young's Modulus	1.38×10^{11}	1.20×10^{11}	Pa
Density	$1,500$	970	$\mathrm{kg/m^3}$

Mass of a Single Rod

The mass required of a single carbon-fiber rod to take the compressive load F subject to buckling constraints without considering gravity is: $m_{rod} = 2\rho_b H^2(\frac{F}{\pi E_b})^{\frac{1}{2}} = 2 \times 1500 \times 2000^2 \times (\frac{9720}{3.14 \times 1.38 \times 10^{11}})^{\frac{1}{2}}$ kg $= 1.7973 \times 10^6$ kg. Considering gravity, we put half of the gravity force $F_{rod} = \frac{1}{2} m_{rod} g_{moon}$ on the top of the rod (the compressive load becomes $F + F_{rod}$), then update the required mass m_{rod} and F_{rod}, keep the iteration until the mass converges, we get $m_{rod,g} = 2.6919 \times 10^8$ kg.

Mass of Tensegrity Structures

To better illustrate the design idea, we reduce the variables of the design. That is, we propose the final configuration of the T-Bar and D-Bar angles of $T_q D_1$ tower to be $\alpha_T = \pi/3$ and $\alpha_D = \pi/18$. The optimization variables for the tower design are structure complexity, cross-sectional area of the members, and prestress in the strings. Algorithm 1 was used in calculating the optimization variables to stabilize and minimize the total structure mass. The results are shown in Table 2. Results show that $q = 2$ with a lower bound of prestress in the strings to guarantees structure stability $\epsilon = 0.46$ is the optimal structure complexity with a total structure mass of 1.4081×10^6 kg. The detail information of the bars and strings are given in Table 3 and the structure configuration is shown in Figure 5.

Table 2: Minimal mass of $T_q D_1$ tensegrity tower and prestress ϵ, $\alpha_T = \pi/3$ and $\alpha_D = \pi/18$.

Structure Complexity	Structure Mass (kg)	Prestress ϵ (N/m)
$q = 1$	1.7400×10^6	0.18
$q = 2$	1.4081×10^6	0.46
$q = 3$	1.9683×10^6	2.10

Table 3: Structure member information of the T_2D_1 tensegrity tower.

Structure Member	Value	Units
Bars Mass	1.4081×10^6	kg
Strings Mass	6.7733	kg
Total Mass	1.4081×10^6	kg

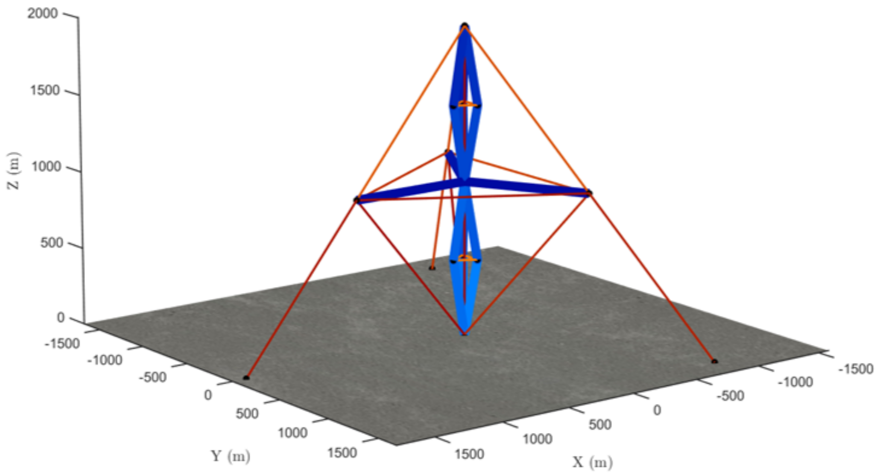

Figure 5: Three-dimensional T_2D_1 Bar structure with force F applied at the top node and bottom nodes fixed. Maroon lines are strings and blue lines are bars, their thickness are scaled accordingly.

CONCLUSIONS

This paper presents a general framework to design minimal mass tensegrity towers. Starting from the compact matrix form of tensegrity statics, we first formulate structure mass subject to yielding and buckling of the structure members. Then, we model the gravitational force by equally distributing the total mass of the member on both end-nodes. The global stiffness matrix is also considered to guarantee the global stability of the structure. Then, we show the minimal mass problems can be formed as a non-linear programming problem, and an algorithm to solve this problem is also discussed. Finally, a case study is presented to design a deployable tensegrity tower. For a 2 km tall tensegrity tower made of carbon rods and UHMWPE strings to support 6000 kg payload in the presence of lunar gravity, T_2D_1 tower gives the minimal mass, 1.4081×10^6 kg, which is 0.52% mass of a single 2 km rod $m_{rod,g} = 2.6919 \times 10^8$ kg to support the same payload. The principles developed in this paper are also applicable to design many other static tensegrity structures.

ACKNOWLEDGEMENT

Some of the work in this paper was partially supported by the National Science Foundation under Award No. NSF CMMI-1634590 and by Texas A&M University. The experimental model, shown in Figure 3b, was supported by a NIAC (NASA Innovative Advanced Concepts) phase I project, Lunar-Polar Propellant Mining Outpost (LPMO): Affordable Exploration and Industrialization, with partner Joel Sercel. The authors appreciate Mr. Ali Hasnain Khowaja for his help in building the experimental model.

References

Abdallah, M. E., Platt, R., Hargrave, B., and Permenter, F. (2012). "Position control of tendon-driven fingers with position controlled actuators." *2012 IEEE International Conference on Robotics and Automation*, IEEE, 2859–2864.

Bliss, T., Werly, J., Iwasaki, T., and Bart-Smith, H. (2012). "Experimental validation of robust resonance entrainment for cpg-controlled tensegrity structures." *IEEE Transactions On Control Systems Technology*, 21(3), 666–678.

Booth, J. W., Cyr-Choiniere, O., Case, J. C., Shah, D., Yuen, M. C., and Kramer-Bottiglio, R. (2020). "Surface actuation and sensing of a tensegrity structure using robotic skins." *Soft Robotics*.

Bundhoo, V., Haslam, E., Birch, B., and Park, E. J. (2009). "A shape memory alloy-based tendon-driven actuation system for biomimetic artificial fingers, part i: design and evaluation." *Robotica*, 27(1), 131–146.

Chen, L.-H., Kim, K., Tang, E., Li, K., House, R., Zhu, E. L., Fountain, K., Agogino, A. M., Agogino, A., Sunspiral, V., and Jung, E. (2017). "Soft spherical tensegrity robot design using rod-centered actuation and control." *Journal of Mechanisms and Robotics*, 9(2), 025001.

Chen, M., Goyal, R., Majji, M., and Skelton, R. E. (2020a). "Design and analysis of a growable artificial gravity space habitat." *Aerospace Science and Technology*, 106, 106147.

Chen, M., Liu, J., and Skelton, R. E. (2020b). "Design and control of tensegrity morphing airfoils." *Mechanics Research Communications*, 103480.

Chen, M., Shen, Y., Goyal, R., Majji, M., and Skelton, R. E. (2018). "Energy analysis of growth adaptable artificial gravity space habitat." *2018 AIAA SPACE and Astronautics Forum and Exposition*, 5109.

Chen, M. and Skelton, R. E. (2020). "A general approach to minimal mass tensegrity." *Composite Structures*, 112454.

Crawford, I. A. (2015). "Lunar resources: A review." *Progress in Physical Geography*, 39(2), 137–167.

Duke, M., Gustafson, R., and Rice, E. (1998). "Mining of lunar polar ice." *36th AIAA Aerospace Sciences Meeting and Exhibit*, 1069.

Fabbrocino, F., Modano, M., Farina, I., Carpentieri, G., and Fraternali, F.

(2017). “Optimal prestress design of composite cable-stayed bridges.” *Composite Structures*, 169, 167–172.

Fuller, R. B. (1959). “Tensile integrity structures. US Patent 3.063.521.

Goyal, R., Chen, M., Majji, M., and Skelton, R. E. (2019). “Motes: Modeling of tensegrity structures.” *Journal of Open Source Software*, 4(42), 1613.

Goyal, R., Hernandez, E. A. P., and Skelton, R. E. (2018). “Analytical study of tensegrity lattices for mass-efficient mechanical energy absorption.” *International Journal of Space Structures*.

Goyal, R. and Skelton, R. E. (2019). “Tensegrity system dynamics with rigid bars and massive strings.” *Multibody System Dynamics*, 46(3), 203–228.

Heiken, G. H., Vaniman, D. T., and French, B. M. (1991). “Lunar sourcebook-a user’s guide to the moon.” *Research supported by NASA,. Cambridge, England, Cambridge University Press, 1991, 753 p. No individual items are abstracted in this volume.*

Kim, H.-I., Han, M.-W., Song, S.-H., and Ahn, S.-H. (2016). “Soft morphing hand driven by sma tendon wire.” *Composites Part B: Engineering*, 105, 138–148.

Ma, S., Chen, M., and Skelton, R. E. (2020). “Design of a new tensegrity cantilever structure.” *Composite Structures*, 112188.

Nagase, K. and Skelton, R. (2014). “Minimal mass tensegrity structures.” *Journal of The International Association for Shell and Spatial Structures*, 55(1), 37–48.

Pike, R. J. (1974). “Depth/diameter relations of fresh lunar craters: Revision from spacecraft data.” *Geophysical Research Letters*, 1(7), 291–294.

Rimoli, J. J. and Pal, R. K. (2017). “Mechanical response of 3-dimensional tensegrity lattices.” *Composites Part B: Engineering*, 115, 30–42.

Rostami, J., Dreyer, C., and Blair, B. (2018). “Lunar tunnel boring machines.” *Earth and Space 2018: Engineering for Extreme Environments*, American Society of Civil Engineers Reston, VA, 240–252.

Sabelhaus, A. P., Akella, A. K., Ahmad, Z. A., and SunSpiral, V. (2017). “Model-predictive control of a flexible spine robot.” *2017 American Control Conference (ACC)*, IEEE, 5051–5057.

Sanders, G. (2019). “Nasa Lunar ISRU Strategy.

Schlaich, M. (2004). “The messeturm in rostockâ–“a tensegrity tower.” *Journal of the International Association for Shell and Spatial Structures*, 45(2), 93–98.

Schrunk, D., Sharpe, B., Cooper, B. L., and Thangavelu, M. (2007). *The moon: Resources, future development and settlement*. Springer Science & Business Media.

Shen, Y., Chen, M., Majji, M., and Skelton, R. E. (2020). “Markov data-based reference tracking of tensegrity morphing airfoils.” *arXiv preprint arXiv:2010.10710*.

Skelton, R. E. and de Oliveira, M. C. (2009). *Tensegrity Systems*. Springer US.

Spudis, P., Bussey, D., Baloga, S., Cahill, J., Glaze, L., Patterson, G., Raney, R., Thompson, T., Thomson, B., and Ustinov, E. (2013). “Evidence for water ice on the moon: Results for anomalous polar craters from the lro mini-rf imaging radar.” *Journal of Geophysical Research: Planets*, 118(10), 2016–2029.

Sultan, C. (2014). “Tensegrity deployment using infinitesimal mechanisms.”

International Journal of Solids and Structures, 51(21-22), 3653–3668.
Sultan, C. and Skelton, R. (2003). “Deployment of tensegrity structures.” *International Journal of Solids and Structures*, 40(18), 4637–4657.
SunSpiral, V., Gorospe, G., Bruce, J., Iscen, A., Korbel, G., Milam, S., Agogino, A., and Atkinson, D. (2013). “Tensegrity based probes for planetary exploration: Entry, descent and landing (edl) and surface mobility analysis.” *International Journal of Planetary Probes*, 7, 13.
Tukkaraja, P., Cross, W., Ajitha, S. S., and Jasthi, B. (2018). “Lunar mining and processing for in situ resource utilization.” *Earth and Space 2018: Engineering for Extreme Environments*, American Society of Civil Engineers Reston, VA, 401–413.
Wang, K., Aanjaneya, M., and Bekris, K. (2020). “An end-to-end differentiable but explainable physics engine for tensegrity robots: Modeling and control.” *arXiv preprint arXiv:2011.04929*.
Yildiz, K. and Lesieutre, G. A. (2018). “A novel deployment strategy for tensegrity towers.” *2018 AIAA Spacecraft Structures Conference*, 0693.
Yildiz, K. and Lesieutre, G. A. (2019). “Effective beam stiffness properties of n-strut cylindrical tensegrity towers.” *AIAA Journal*, 57(5), 2185–2194.
Zhao, L. and Hernandez, E. A. P. (2019). “Theoretical study of tensegrity systems with tunable energy dissipation.” *Extreme Mechanics Letters*, 32, 100567.